Renormalization of nanoparticle polarizability in the vicinity of a graphene-covered interface

Jaime E. Santos,[*] M. I. Vasilevskiy, N. M. R. Peres, G. Smirnov, and Yu. V. Bludov

Centro de Física and Departamento de Física, Universidade do Minho, P-4710-057 Braga, Portugal

We study the electromagnetic properties of a metamaterial consisting of polarizable (nano)particles and a single graphene sheet placed at the interface between two dielectrics. We show that the particle's polarizability is renormalized because of the electromagnetic coupling to surface plasmons supported by graphene, which results in a dispersive behavior, different for the polarizability components corresponding to the induced dipole moment, parallel and perpendicular to the graphene sheet. In particular, this effect is predicted to take place for a metallic particle whose bare polarizability in the terahertz (THz) region is practically equal to the cube of its radius (times $4\pi\varepsilon_0$). This opens the possibility to excite surface plasmons in graphene and enhance its absorption in the THz range by simply using a monolayer of metallic particles randomly deposited on top of it, as we show by explicit calculations.

I. INTRODUCTION

Electromagnetic (EM) metamaterials are artificial structures designed in such a way that their optical properties differ from those existing in natural materials [1,2]. They offer new functionalities, such as radiation guiding [3], enhanced absorption and EM energy concentration in subwavelength regions [4,5], extraordinary transmission [6], color filtering [7] and tailoring [8], surface-enhanced Raman scattering (SERS) [9], etc. Many of these unusual properties are related to surface plasmons, collective oscillations of free electrons, which either propagate along a conductor's surface or a nanowire, or are localized in a metallic nanoparticle (NP) [10,11]. Graphene, a two-dimensional conductor, possesses unusual electronic properties [12], and graphene plasmonics [13] has become a field of intense research, both theoretical and experimental; see Refs. [14,15] for reviews. It offers the possibility of expansion of metamaterials to the far-infrared (FIR) and THz spectral range and allows for their tunability, most directly achieved by adjusting the Fermi level in graphene through an external gate voltage [16], but also in a number of different ways, which can be implemented by using periodic structures of graphene ribbons [17,18], two- [19–21] or three-dimensional [22,23] arrays of graphene disks, or a two-dimensional array of antidots [24].

A potentially interesting direction of research is combining graphene with quasi-zero-dimensional emitters or absorbers, such as organic molecules [25–27] or semiconductor quantum dots (QDs) [28,29]. Such study explores the possibilities of electromagnetic coupling between localized excitations (for instance, molecular or QD excitons) and propagating graphene plasmons in order to probe the de-excitation dynamics [25] or dispersion relation of plasmon-polaritons in graphene [27], enhance the Förster transfer between an emitter and an absorber [26], control the coupling between two emitters (superradiance effect) [30], or enhance the EM radiation absorption in graphene [31]. Another possibility that has been recently demonstrated experimentally [32,33] is that of electromagnetic coupling between the said graphene plasmons

and an illuminated atomic force microscope tip, which allows for the study of the plasmon dispersion relation as a function of the gating applied to graphene.

Qualitatively similar effects have been predicted and observed, in the visible range, for hybrid systems with metal plasmons; for instance, generation of single optical plasmons in metallic nanowires coupled to QDs [34], metal-enhanced [35] or quenched [36,37] fluorescence of colloidal semiconductor nanocrystals, or resonant absorption by exciton-plasmon polaritons [38,39]. However, the case of graphene is special not only because it involves a different spectral region, but also because graphene is a semimetal and its plasma oscillations are mediated by both intraband and interband transitions, with a characteristic frequency-dependent conductivity [12]. Moreover, since it is a monolayer-thick material, it should be considered as a two-dimensional (2D) object rather than a very thin 3D film [14]. As a result, graphene, for instance, supports both *p*- and *s*-polarized surface waves [40]. In such a case, the EM coupling to nonplasmonic excitations may also have features that are not known for metal surface plasmons.

The aim of the present paper is to provide both a qualitative and quantitative account of the electromagnetic properties of a metamaterial consisting of polarizable (nano)particles and a single graphene sheet placed at the interface between two dielectrics, one of which incorporates the particles. Using the electrostatic approximation, we calculate the field created by polarization charges induced on the graphene sheet by the particle excited by an external EM field, as well as the said surface charge density on graphene, and describe the resulting effect in terms of its renormalized polarizability. The calculation of the frequency-dependent renormalized polarizability is the main result of this article. We show that it is a second-rank tensor with two unequal principal values, which can have a pronounced dependence upon the excitation frequency even if particle's polarizability is nondispersive in the considered THz spectral range. In particular, this effect is shown to take place for a spherical gold particle lying on the graphene sheet. Once the renormalized polarizability of a single particle is computed, the EM properties (i.e., reflection, transmission and absorption spectra) of the metamaterial consisting of a graphene layer sandwiched between two dielectrics, one of which is doped with polarizable particles,

---

*jaime.santos@fisica.uminho.pt

can be calculated. We explicitly compute the THz optical properties of a monolayer of nonabsorbing nanoparticles randomly deposited on top of a graphene sheet and show that the absorption in graphene is enhanced due to the excitation of surface plasmons.

This article is organized as follows. In Sec. II, we define our model system and derive the electrostatic boundary conditions on graphene. The electric fields are obtained using the method of images in Sec. III. In Sec. IV, the renormalized polarizability is introduced and a few examples, involving nanoparticles constituted of different materials, are also discussed. The following two sections present the calculated results for the polarization charge density induced on graphene and the THz optical spectra of the system composed of a monolayer of polarizable particles randomly deposited on the graphene sheet. We conclude in Sec. VII.

II. MODEL SYSTEM AND ASSOCIATED BOUNDARY CONDITIONS

We first consider the problem of a single polarizable (nano)particle, placed in the vicinity of the interface between two dielectrics, with relative permittivities that can depend on the frequency ω of the electric field in the media, given by $\varepsilon_1(\omega)$ (in medium 1, the upper medium) and $\varepsilon_2(\omega)$ (in medium 2, the lower medium). The particle is located in medium 1 at a distance h along the normal to the interface, the interface being identified with the plane $z = 0$ in our system of coordinates [the position of the particle is given by $\mathbf{r}_0 = (0,0,h)$; see Fig. 1]. The interface is constituted by a graphene sheet, which is homogeneous in a macroscopic scale and is described at this scale by its (frequency-dependent) conductivity $\sigma(\omega)$. We will treat the problem in the electrostatic approximation where one can neglect both the retardation effects and the magnetic field associated with the electric field present in the media. Thus, in both media, the electric field is given by $\mathbf{E} = -\nabla\phi(\mathbf{r},\omega)$, where $\phi(\mathbf{r},\omega)$ is the electric scalar potential. Since the location of the dipole along the xy plane can be chosen arbitrarily, it is appropriate to perform a partial Fourier transform from real space to the reciprocal space of the wave vector $\mathbf{q} = (q_x, q_y)$, keeping however the dependency of ϕ on the z coordinate [41].
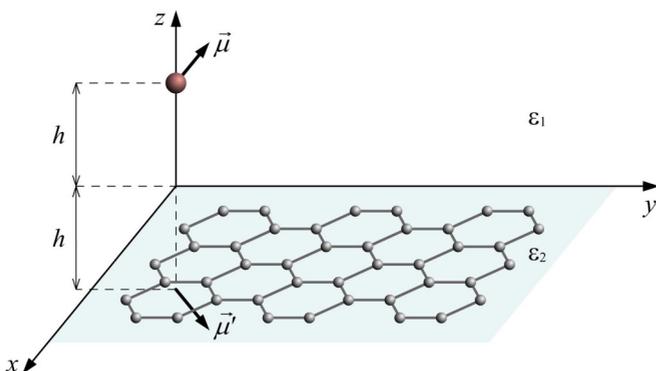
FIG. 1. (Color online) Schematics of the system consisting of a dipole (polarized NP) located at a point $(0,0,h)$ in the vicinity of a graphene-covered interface between two dielectrics. An image dipole located at $(0,0,-h)$ is also shown.

In medium 1, the electric potential obeys Poisson's equation with a source term that describes the presence of the polarizable nanoparticle, modeled as an electric dipole of magnitude $\boldsymbol{\mu}$, which we will later set to be proportional to the applied field. In medium 2, the electric potential obeys Laplace's equation. One relates the field in the two media through the boundary condition that determines the discontinuity in the normal component of the electric displacement vector, $\mathbf{D} = \varepsilon_0 \varepsilon \mathbf{E}$, across the interface. Such a boundary condition reads, after Fourier transformation,

$$\varepsilon_1(\omega)\frac{\partial\phi(z,\mathbf{q},\omega)}{\partial z}\bigg|_{z=0^+} - \varepsilon_2(\omega)\frac{\partial\phi(z,\mathbf{q},\omega)}{\partial z}\bigg|_{z=0^-}$$
$$= -\frac{\delta\rho(\mathbf{q},\omega)}{\varepsilon_0}, \qquad (1)$$

where ε_0 is the vacuum permittivity and $\delta\rho(\mathbf{q},\omega)$ is the surface density of charge induced in the graphene sheet. It is related to the current density, $\boldsymbol{J}(\mathbf{q},\omega)$, in the graphene sheet by the continuity equation

$$\omega\,\delta\rho(\mathbf{q},\omega) = \mathbf{q}\cdot\boldsymbol{J}(\mathbf{q},\omega). \qquad (2)$$

In order to close the system of equations necessary for the solution of the problem, we need the equation that relates the surface density of current to the local electric field present in the graphene sheet. Within the realm of a diffusion-drift model that describes the graphene sheet, one has:

$$\boldsymbol{J}(\mathbf{q},\omega) = -i\sigma(\omega)\mathbf{q}\left(\phi(z=0,\mathbf{q},\omega) + \frac{1}{e^2}\frac{\partial E_F}{\partial n}\frac{\delta\rho(\mathbf{q},\omega)}{1-i\omega\tau_F}\right), \qquad (3)$$

where the derivative $\frac{\partial E_F}{\partial n}$, with E_F being the Fermi energy of graphene and n the density of carriers, is computed at thermal equilibrium and is given, at zero temperature, by $\frac{\partial E_F}{\partial n} = \rho^{-1}(E_F)$; i.e., this quantity is just the inverse density of states of graphene at the Fermi level. Finally, τ_F denotes the quasiparticles' relaxation time that enters the Drude formula of the conductivity (see below). This formula also shows that it is possible to neglect the diffusion term with respect to the drift one in the limit of $\omega\tau_F \gg 1$.

Substituting (3) in (2) and introducing the diffusion constant of carriers in graphene through

$$D(\omega) = \frac{\sigma(\omega)}{e^2(1-i\omega\tau_F)}\frac{\partial E_F}{\partial n} = \frac{v_F^2\tau_F}{2(1-i\omega\tau_F)^2}, \qquad (4)$$

where we have used the Drude form for the conductivity of graphene [14], $\sigma(\omega) = \sigma_0/(1-i\omega\tau_F)$, with $\sigma_0 = \frac{1}{2}e^2 v_F^2\tau_F\rho(E_F)$, with v_F being graphene's Fermi's velocity, we obtain

$$\delta\rho(\mathbf{q},\omega) = -\frac{\sigma(\omega)q^2}{-i\omega + D(\omega)q^2}\phi(z=0,\mathbf{q},\omega), \qquad (5)$$

which relates the local density of charge in the graphene sheet with the local value of the electric potential. Substituting this equation in (1), we obtain the relation

$$\varepsilon_1(\omega)\frac{\partial\phi(z,\mathbf{q},\omega)}{\partial z}\bigg|_{z=0^+} - \varepsilon_2(\omega)\frac{\partial\phi(z,\mathbf{q},\omega)}{\partial z}\bigg|_{z=0^-}$$
$$= \frac{\sigma(\omega)q^2}{\varepsilon_0(-i\omega + D(\omega)q^2)}\phi(z=0,\mathbf{q},\omega), \qquad (6)$$

which is in a form that involves the electric potential alone. One needs to add to (6) the condition of continuity of the potential at the graphene sheet,

$$\phi(z = 0^-, \mathbf{q}, \omega) = \phi(z = 0^+, \mathbf{q}, \omega), \tag{7}$$

equivalent to the condition of continuity of the transverse components of the electric field and necessary for (6) to be properly defined. The solution of Poisson's equation in medium 1, with a source term representing the electric dipole, and of Laplace's equation in medium 2, with both solutions satisfying the boundary conditions (6) and (7), constitutes the mathematical solution of our physical problem, to which we turn to in the next section.

III. SOLUTION BY METHOD OF IMAGES IN RECIPROCAL SPACE

In the absence of the graphene sheet, the problem described above is solvable through the method of images [42]. In medium 1, the electric potential is given by the superposition of the potential created by the original dipole and that of an image dipole of appropriate strength, $\boldsymbol{\mu}' = A[2(\boldsymbol{\mu} \cdot \hat{\mathbf{z}})\hat{\mathbf{z}} - \boldsymbol{\mu}]$, located at $-\mathbf{r}_0 = (0, 0, -h)$, where $\hat{\mathbf{z}}$ is the unit vector in the direction perpendicular to the interface. In medium 2, the potential is that of a dipole placed at $\mathbf{r}_0$ in medium 1, but with a strength that is different in magnitude from that of the original dipole, $\boldsymbol{\mu}'' = B\boldsymbol{\mu}$. In the mixed real-space/reciprocal-space representation used above, the solution of the problem in the absence of the graphene sheet is given, in regions 1 and 2, by

$$\phi_1(z, \mathbf{q}, \omega) = \frac{1}{2\varepsilon_0 \varepsilon_1} \left[A[(\boldsymbol{\mu} \cdot \hat{\mathbf{z}}) + i\boldsymbol{\mu} \cdot \hat{\mathbf{q}}] e^{-q(z+h)} \right.$$
$$\left. + [(\boldsymbol{\mu} \cdot \hat{\mathbf{z}}) \text{sgn}(z - h) - i\boldsymbol{\mu} \cdot \hat{\mathbf{q}}] e^{-q|z-h|} \right], \tag{8}$$

$$\phi_2(z, \mathbf{q}, \omega) = -\frac{B}{2\varepsilon_0 \varepsilon_2} [(\boldsymbol{\mu} \cdot \hat{\mathbf{z}}) + i\boldsymbol{\mu} \cdot \hat{\mathbf{q}}] e^{q(z-h)}, \tag{9}$$

where $\hat{\mathbf{q}}$ is the unit vector along $\mathbf{q}$.

In order to generalize this solution to the case where the graphene sheet is present at the interface, all one has to do is to consider the coefficients A and B as functions of $\mathbf{q}$. Substituting the solutions (8) and (9) in the boundary conditions (6) and (7) yields

$$A(q, \omega) = \frac{\varepsilon_2 - \varepsilon_1 + f(q, \omega)}{\varepsilon_1 + \varepsilon_2 + f(q, \omega)}, \tag{10}$$

$$B(q, \omega) = \frac{2\varepsilon_2}{\varepsilon_1 + \varepsilon_2 + f(q, \omega)}, \tag{11}$$

where

$$f(q, \omega) = \frac{q\sigma(\omega)}{\varepsilon_0[-i\omega + D(\omega)q^2]}. \tag{12}$$

Equations (8) and (9), with $A(q, \omega)$ and $B(q, \omega)$ given, respectively, by (10) and (11), constitute the general solution of the considered problem within the realm of the electrostatic approximation.

IV. RENORMALIZED POLARIZABILITY

A. General expressions

We now consider that a homogeneous electric field $\mathbf{E}^0(\omega)$ is applied to the system. In the absence of the graphene sheet and for $\varepsilon_2 = \varepsilon_1$, the particle would respond to such a field by developing an electric dipole moment $\boldsymbol{\mu} = \varepsilon_1 \alpha_0(\omega) \mathbf{E}^0$, where $\alpha_0(\omega)$ is the particle's polarizability [10], which depends on the material nature and geometry of the particle as well as on ε_1. We shall consider it as a scalar function of frequency. In the situation depicted in Fig. 1, we have

$$\boldsymbol{\mu} = \varepsilon_1 \alpha_0(\omega) \mathbf{E}^l, \tag{13}$$

where $\mathbf{E}^l = \mathbf{E}^0 - \nabla\phi_{\text{pol}}$ and ϕ_{pol} is the potential created by the polarization charges at the interface, i.e., excluding the self-field created by the nanoparticle, which is represented by the first term of Eq. (8). Expressing the dipole moment (13) in terms of $\mathbf{E}^0$, we define the renormalized polarizability [43]

$$\boldsymbol{\mu} = \varepsilon_1 \boldsymbol{\alpha}^*(\omega) \cdot \mathbf{E}^0, \tag{14}$$

where the quantity $\boldsymbol{\alpha}^*(\omega)$ is a second-rank tensor. The electric potential ϕ_{pol} is given, in real space and in medium 1, by

$$\phi_{\text{pol}}(\mathbf{r}, \omega) = \frac{1}{2\varepsilon_0 \varepsilon_1} \int \frac{d^2q}{(2\pi)^2} e^{i\mathbf{q} \cdot \boldsymbol{\rho}}$$
$$\times A(q, \omega) [(\boldsymbol{\mu} \cdot \hat{\mathbf{z}}) + i\boldsymbol{\mu} \cdot \hat{\mathbf{q}}] e^{-q(z+h)}, \tag{15}$$

where $\boldsymbol{\rho} = (x, y)$ and $A(q, \omega)$ is given by (10).

Applying the gradient operator under the integration sign and substituting (13), we obtain for the local field acting on the particle

$$\mathbf{E}^l(\omega) = \mathbf{E}^0(\omega) + \frac{\alpha_0(\omega)}{2\varepsilon_0} \int \frac{d^2q}{(2\pi)^2} q e^{-2qh} A(q, \omega)$$
$$\times (E_z^l \hat{\mathbf{z}} + (\mathbf{E}^l \cdot \hat{\mathbf{q}}) \hat{\mathbf{q}}). \tag{16}$$

Since $A(q, \omega)$ only depends on the modulus of $\mathbf{q}$, one can easily perform the angular integrals in (16), which yields

$$\mathbf{E}^l(\omega) = \mathbf{E}^0(\omega) + \frac{\alpha_0(\omega)}{8\pi\varepsilon_0} a(h, \omega) (2E_z^l \hat{\mathbf{z}} + E_x^l \hat{\mathbf{x}} + E_y^l \hat{\mathbf{y}}), \tag{17}$$

where $\hat{\mathbf{x}}$ and $\hat{\mathbf{y}}$ are the unit vectors in the directions of the interface and

$$a(h, \omega) = \int_0^\infty dq \, q^2 e^{-2qh} A(q, \omega). \tag{18}$$

Using the components of this equation to express $\mathbf{E}^l$ in terms of $\mathbf{E}^0$, substituting in (13) and comparing with (14), we obtain the following expressions for the principal components of the tensor $\boldsymbol{\alpha}^*$:

$$\alpha_{xx}^*(\omega) = \alpha_{yy}^*(\omega) = \frac{\alpha_0(\omega)}{1 - \frac{\alpha_0(\omega)}{8\pi\varepsilon_0} a(h, \omega)}, \tag{19}$$

$$\alpha_{zz}^*(\omega) = \frac{\alpha_0(\omega)}{1 - \frac{\alpha_0(\omega)}{4\pi\varepsilon_0} a(h, \omega)}. \tag{20}$$

At sufficiently high frequencies, we can neglect the diffusion term [i.e., we can set $D(\omega) = 0$] in the expressions above,

reducing $a(h,\omega)$ to the following form:

$$a(h,\omega) = \frac{1}{4h^3}\left(1 + \frac{\beta_1}{1+\varepsilon_2/\varepsilon_1} + \frac{\beta_1^2}{1+\varepsilon_2/\varepsilon_1}\right.$$
$$\left. + \frac{\beta_1^3}{1+\varepsilon_2/\varepsilon_1} \, e^{-\beta_1} \left[-\text{Ei}(\beta_1) + i\pi\right]\right), \quad (21)$$

where $\beta_1 = i\frac{2\omega\varepsilon_0 h(\varepsilon_1+\varepsilon_2)}{\sigma(\omega)}$ and $\text{Ei}(\beta_1) = -P\int_{-\beta_1}^{\infty} dx\,\frac{e^{-x}}{x}$ is the exponential integral function [44].

We would like to point out the connection between the expression obtained for the renormalized polarizability and the existence of surface plasmon polaritons (SPPs) in graphene. The integral appearing in the definition of the function $a(h,\omega)$, Eq. (18) has the form [45]

$$I = \int_0^{\infty} \frac{\varepsilon_2 - \varepsilon_1 + f(q,\omega)}{\varepsilon_1 + \varepsilon_2 + f(q,\omega)} \, e^{-2qh} q^2 dq. \quad (22)$$

Neglecting the diffusion term, the poles of the integrand are given by the equation

$$\frac{\varepsilon_2 + \varepsilon_1}{q} = \frac{\sigma(\omega)}{i\omega\varepsilon_0}, \quad (23)$$

which is the SPP dispersion relation in the electrostatic approximation [14]. The SPP wavevector for a given ω, q_1, determines the dependence of $a(h,\omega)$ upon the distance between the particle and the graphene sheet, h, since $\beta_1 = 2q_1 h$ in Eq. (21).

B. Examples

For a spherical particle of a radius R, made of a dispersive material with a dielectric function $\varepsilon_3(\omega)$, we have [42]

$$\alpha_0(\omega) = 4\pi\varepsilon_0 \frac{\varepsilon_3(\omega) - \varepsilon_1}{\varepsilon_3(\omega) + 2\varepsilon_1} R^3. \quad (24)$$

This formula can describe a simple dielectric inclusion, a metallic particle [11], if $\varepsilon_3(\omega) = \varepsilon_\infty + i\sigma_{3D}(\omega)/(\varepsilon_0\omega)$ with ε_∞ denoting the background dielectric permittivity and σ_{3D} the optical conductivity of a bulk metal and also, with some modification, a semiconductor QD [39]. For a particle made of a typical metal, such as gold, with the plasma frequency lying in the UV spectral region, we have $\varepsilon_3(\omega) \gg 1$ and $\alpha_0 \approx 4\pi\varepsilon_0 R^3$ in the THz range, i.e., the bare polarizability is nearly real and dispersionless.

Note that for a spherical particle, one obtains, by setting $\sigma(\omega) = 0$ in (10) and substituting the result in (18) (i.e., in the absence of graphene), the formula

$$a(h,\omega) = \frac{1}{4h^3} \frac{\varepsilon_2 - \varepsilon_1}{\varepsilon_2 + \varepsilon_1} \quad (25)$$

and the expressions for the components of α^*, (19) and (20), coincide with those obtained in Ref. [43].

Considering the Drude form of the optical conductivity of graphene, introduced in Eq. (4) above, we have that, in the limit of high frequencies, the real part of the conductivity is small with respect to the imaginary part. Assuming also that ε_1 and ε_2 are real constants, the dispersion relation (23) yields $\omega \propto \sqrt{q}$. The renormalized polarizability of a gold particle of several microns in size is shown in Fig. 2. It shows a Lorentzian-type dispersion induced by the polarization of graphene, larger for
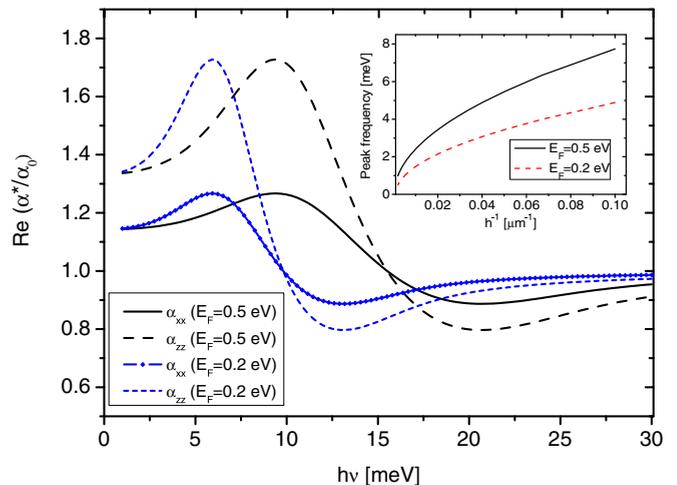
FIG. 2. (Color online) Frequency dependence of the real part of the renormalized polarizability components (divided by the bare one, α_0) for a spherical Au particle of radius $R = 10\,\mu$m located at a distance $h = 10\,\mu$m from a suspended graphene sheet ($\varepsilon_2 = \varepsilon_1 = 1$), for two values of the Fermi level as indicated. The inset shows the peak frequency dependence on the inverse of the particle's distance from the graphene sheet. Gold parameters are taken from Ref. [8].

the "normal" (zz) component. The position of the peak depends on the distance and the dependence on h^{-1} resembles the SPP dispersion as can be seen in the inset of Fig. 2. We can say that the renormalized polarizability presents a resonance due to the excitation of SPPs in graphene, with the wave vector $q \sim h^{-1}$. The other components of α^* show a similar behavior but the amplitude of the resonance is smaller. The same conclusions are valid for particles made of a dispersionless dielectric or even for a spherical cavity in one of the dielectrics surrounding the graphene sheet; however, the coupling is weaker in these cases.

An interesting situation arises when the particle's bare polarizability has its own resonance; for instance, if it is made of a polar semiconductor, for example CdSe, with a characteristic reststrahlen band between the transverse (ω_{TO}) and longitudinal (ω_{LO}) optical phonon frequencies, with the dielectric function given by [46]

$$\varepsilon_3(\omega) = \varepsilon_\infty\left(1 + \frac{\omega_{LO}^2 - \omega_{TO}^2}{\omega_{TO}^2 - \omega^2 - i\omega\Gamma_{TO}}\right), \quad (26)$$

where $\varepsilon_\infty = \text{const}$ and Γ_{TO} is the phonon damping. The polarizability of such a particle shows a Lorentzian-type dispersion [see Fig. 3(a)]. In this case, a double resonance can occur when the SPP frequency (determined by the wave vector $q \sim h^{-1}$) falls within the reststrahlen band (between ω_{TO} and ω_{LO}) and the denominator in Eq. (20) [or Eq. (19)] is small. Although such a resonance is strongly damped because of the large value of Im α_0, its presence results in a considerable enhancement of the imaginary part of the polarizability, which represents an additional absorption for the particle when located close to the graphene sheet [see Fig. 3(a)]. We also note that the peak frequency shifts slightly downwards.

For a fixed frequency, the renormalized polarizability components show a nontrivial dependence upon the Fermi
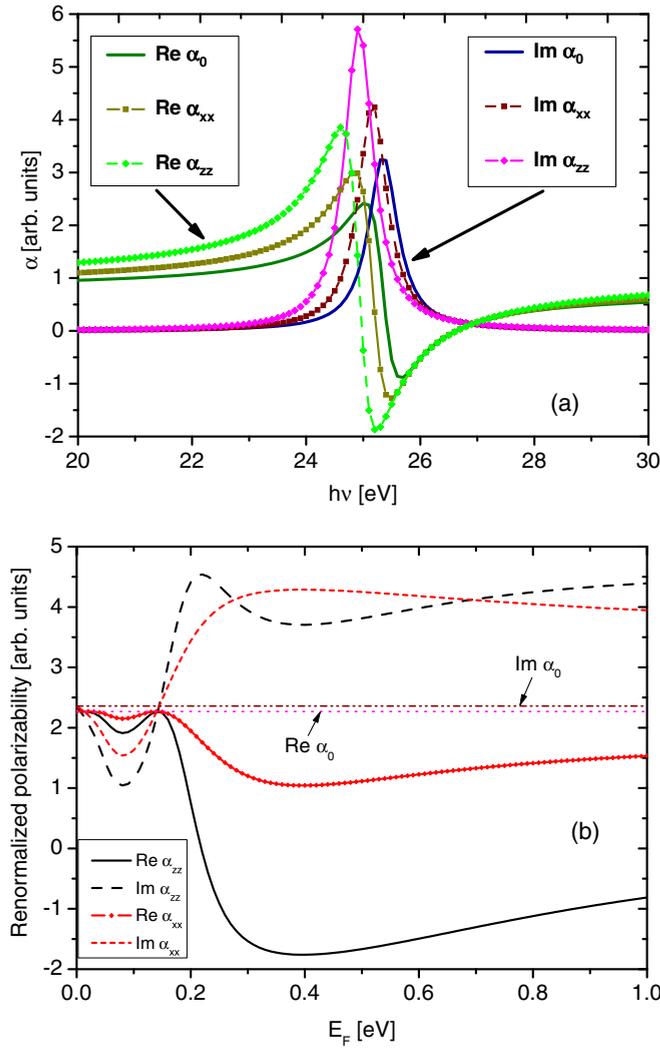
FIG. 3. (Color online) Dependence of the real and imaginary parts of the renormalized polarizability components on the frequency (a) and the Fermi level (b), calculated for a spherical CdSe particle of radius $R = 1 \mu m$ located at a distance $h = 1.1 \mu m$ from a suspended graphene sheet ($\varepsilon_2 = \varepsilon_1 = 1$). The graphene Fermi level is $E_F = 0.4$ eV for (a) and the field frequency is $\hbar\omega_0 = 25.15$ meV for (b). Panel (a) also shows the frequency dependence of the bare polarizability, α_0. Thin horizontal lines in panel (b) indicate the values of the real and imaginary parts of α_0 for $\hbar\omega_0 = 25.15$ meV. Phonon parameters of CdSe were taken from Ref. [47].

level [see Fig. 3(b)], with the absorption enhancement taking place above a certain value [$E_F \approx 0.16$ eV in Fig. 3(b)]. In order to understand this behavior, we recall that the polarizability enhancement factor depends on E_F through Eq. (21) and that

$$\beta_1 \approx \frac{2\omega\varepsilon_0(\varepsilon_1 + \varepsilon_2)}{\text{Im}\,\sigma}h, \qquad (27)$$

with $\text{Im}\,\sigma \approx 4\alpha_F \varepsilon_0 E_F/(\hbar\omega)$ (where α_F is the fine structure constant), i.e., $\beta_1 \propto (\hbar\omega/E_F)$. We would recognize in the variation of the real part of the renormalized polarizability seen in Fig. 3(b) the same dispersive behavior seen in Fig. 2, if we were to represent the functions plotted in this latter

figure in terms of ω^{-1}, rather than ω. The characteristic value of E_F corresponds to the matching of the SPP frequency (at $q \sim h^{-1}$) with the phonon resonance frequency. In principle, such a pronounced dependence of $\text{Im}\,\alpha^*$ upon E_F opens the possibility to probe the Fermi level in gated graphene by measuring the resonant absorption of radiation by such particles. Note that such a double resonance should occur whenever $\alpha_0(\omega)$ shows a strong dispersion. For instance, for a QD, the real part of the bare polarizability, $\text{Re}\,\alpha_0(\omega)$, strongly oscillates in the vicinity of the excitonic transitions, and if the dot is made of a narrow gap material (e.g., PbTe) a coupling between a confined QD exciton and surface plasmon waves can take place [39].

V. POLARIZATION CHARGE ON GRAPHENE

Once the renormalized polarizability components are known, one can compute the induced surface charge density $\delta\rho(\boldsymbol{\rho},\omega)$ on the graphene sheet by computing the inverse Fourier transform of (5), with $\phi(z = 0, \mathbf{q}, \omega)$ given by Eq. (9), where $B(q,\omega)$ is defined by (11). This yields, with $D(\omega) = 0$,

$$\delta\rho(\boldsymbol{\rho},\omega) = \varepsilon_1 \int \frac{d^2q}{(2\pi)^2} \frac{q^2 e^{i\mathbf{q}\cdot\boldsymbol{\rho}-qh}}{q - q_1} \Big[\alpha_{zz}^*(\omega) E_z^0(\omega)$$
$$+ i\,\alpha_{xx}^*(\omega)(\hat{\mathbf{q}}\cdot\mathbf{E}^0(\omega)) \Big], \qquad (28)$$

where $q_1 = \beta_1/(2h)$. Performing the relevant angular integrals, one obtains

$$\delta\rho(\boldsymbol{\rho},\omega) = \frac{\varepsilon_1}{h^3} \Big[\alpha_{zz}^*(\omega)\, E_z^0(\omega)\, g_0(h,\rho,\omega)$$
$$- \alpha_{xx}^*(\omega)\, (\mathbf{E}_\parallel^0(\omega)\cdot\hat{\boldsymbol{\rho}})\, g_1(h,\rho,\omega) \Big], \qquad (29)$$

with dimensionless functions g_0 and g_1 defined as follows:

$$g_n(h,\rho,\omega) = \frac{h^3}{2\pi} \int_0^\infty dq\, \frac{q^3 e^{-qh}}{q - q_1}\, J_n(q\rho), \qquad (30)$$

where $J_n(x)$ is the Bessel function of order $n = 0, 1$, $\mathbf{E}_\parallel^0(\omega)$ is the applied electric field along the interface, and $\hat{\boldsymbol{\rho}}$ is the unit vector along $\boldsymbol{\rho}$. The dependence of the functions g_0 and g_1 upon the distance within the graphene plane is shown in Fig. 4. Note that the first term in Eq. (29) corresponds to an isotropic charge distribution (we can say that it corresponds to an SPP mode with zero angular momentum, $l = 0$), while the second one is proportional to the cosine of the angle between ρ and $\mathbf{E}_\parallel^0$ (we may call it $l = 1$ mode). These oscillations of the charge density are nothing but the surface plasmons with the wave vector q_1. As seen from Fig. 4, the SPP excitation is more efficient if the external field $\mathbf{E}^0$ is normal to the interface, entailing a larger dipole moment and, consequently, a higher surface charge density induced on graphene. The functions g_n decrease rapidly with h (see upper panels in Fig. 4) and at large distances from the interface this decay is approximately $\sim h^{-3}$.

VI. OPTICAL SPECTRA OF A NP-GRAPHENE METAMATERIAL

Finally, let us consider the situation where polarizable particles are randomly dispersed above a graphene-covered dielectric substrate. For the sake of simplicity, we shall
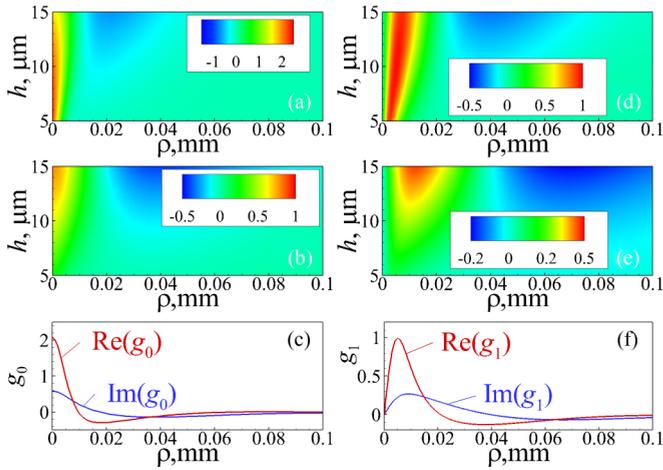
FIG. 4. (Color online) Dependence of the characteristic functions g_0 (left column) and g_1 (right column) that determine the polarization charge density [Eq. (29)] upon height above the interface and the distance from the dipole projection in the graphene plane. Color code plots show the real [(a) and (d)] and imaginary [(b) and (e)] parts of g_0 and g_1 as functions of h and ρ. Plots (c) and (f) are for $h = 10\,\mu$m. The parameters are $\varepsilon_2 = \varepsilon_1 = 1$, $R = 5\,\mu$m, $E_F = 0.5$ eV, $\tau_F = 10^{-13}$ s, $\hbar\omega = 10$ meV.

assume that they form a monolayer, i.e., all the particles are located approximately at the same distance (h) from the surface. Such monolayers of gold or silver particles can be prepared by colloidal chemistry methods [48]. If the typical distances between them are much larger than h, their direct interaction can be neglected and each of the particles can still be described by the renormalized polarizability tensor. If a plane linear-polarized EM wave impinges the system, at normal incidence (see inset in Fig. 5), the total dipole moment of the NP layer (per unit area) is simply given by $P_x = \nu\varepsilon_1\alpha_{xx}^* E_x$, where ν is the number of particles in the monolayer per unit area and E_x is the electric field. In this case, the surface density of the displacement current produced by the time-dependent polarization of the NP layer, $J_x = -i\omega P_x$, can be related to the external field through the effective optical conductivity,

$$\sigma_{NP}^*(\omega) = -i\omega\nu\varepsilon_1\alpha_{xx}^*(\omega). \tag{31}$$

The polarization current yields a discontinuity of the magnetic component of the EM field (H_y), similar to what takes place at a graphene sheet [14],

$$H_y(z = \delta^+) - H_y(z = \delta^-) = \sigma_{NP}^* E_x(z = \delta), \tag{32}$$

while E_x is continuous across the interface [49]. Using these boundary conditions, it is straightforward to obtain the amplitudes of the transmitted and reflected waves (see Appendix B). In the limit $\omega(R + h)/c \ll 1$ the reflection and transmission coefficients (defined as the ratios of the magnetic field amplitudes) are given by

$$\hat{r} = \frac{1 - \sqrt{\varepsilon_2} + \frac{(\sigma + \sigma_{NP}^*)}{\varepsilon_0 c}}{1 + \sqrt{\varepsilon_2} - \frac{(\sigma + \sigma_{NP}^*)}{\varepsilon_0 c}}, \quad \hat{t} = \frac{2\sqrt{\varepsilon_2}}{1 + \sqrt{\varepsilon_2} + \frac{(\sigma + \sigma_{NP}^*)}{\varepsilon_0 c}}. \tag{33}$$
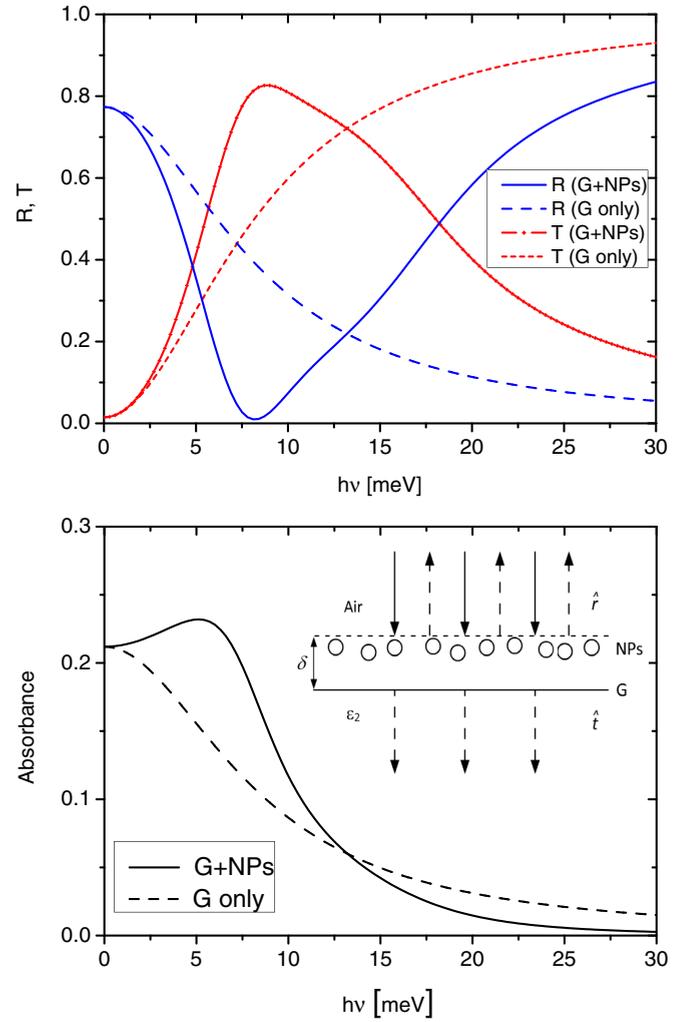
FIG. 5. (Color online) Reflectance, transmittance (a), and absorbance (b) spectra of a monolayer of Au NPs randomly deposited on top of a free-standing graphene sheet. The corresponding spectra of graphene itself are also shown (dashed lines) for comparison. The inset shows the schematics of the considered system. The parameters are the following: $R = 5\,\mu$m, $h = 5\,\mu$m, $E_F = 0.5$ eV, $\nu = 8 \times 10^{-4}\,\mu$m^{-2}.

The experimentally measured reflectance (R) and transmittance of the EM wave are defined as follows [50]:

$$R = |\hat{r}|^2, \quad T = \frac{1}{\sqrt{\varepsilon_2}}|\hat{t}|^2. \tag{34}$$

The absorbance is given by $A = 1 - T - R$.

The quantities R, T, and A are determined directly by the sum of the optical conductivities of graphene and the NP monolayer, ($\sigma + \sigma_{NP}^*$), and the latter takes into account their interaction (the calculated reflectance, transmittance, and absorbance spectra are shown in Fig. 5). As seen from this figure, in the vicinity of the SPP resonance (approximately 8 meV in this case) the reflectivity of the structure falls to nearly zero, while the transmittance is increased, compared to the case of pure graphene-covered interface. This effect can be called plasmon-assisted enhanced transmission. Its physical cause (excitation of surface plasmons) is the same of the

famous extraordinary optical transmission in metallic films with subwavelength hole arrays [6,51]. At the same time, the absorbance is also enhanced in this spectral region and the enhancement factor is nearly 100% close to the resonance frequency [A increases from ≈ 0.13 to ≈ 0.23 at $\omega = 7$ meV in Fig. 5(b)] because SPPs in graphene, excited via NPs, are damped. Note that, as stated above, the bare polarizability of a metallic nanoparticle is (nearly) real. Thus, the rather large imaginary part of its renormalized counterpart is due to the presence of $a(h,\omega)$ in the denominators of equations (19) and (20), and this function only acquires an imaginary part in the presence of graphene, whose coupling to the nanoparticle is responsible for the increased absorbance. This effect can directly be seen in Eq. (33), from which one can compute the absorbance of the system: the largest contribution to this quantity comes from the real part of $\sigma_{NP}^*(\omega)$ [proportional to the imaginary part of $\alpha_{xx}^*(\omega)$], whereas the effect of graphene alone [encoded in $\sigma(\omega)$], is small. As a result, the absorbance of the whole system is enhanced in the vicinity of $\omega(q_1)$. As the frequency increases, the reflectivity grows (and A decreases) due to the increasing optical conductivity of the NP layer [see Eq. (31)].

VII. CONCLUSIONS

In summary, we derived the electric field created by a polarizable particle located in the vicinity of a graphene-covered interface between two dielectrics. We have shown that the particle's polarizability is renormalized because of its interaction with the polarization charges induced on the interface and, in particular, due to the particle's coupling to surface plasmons supported by graphene. As a result, the renormalized polarizability is a tensor with two unequal principal components which depend on the frequency even if the bare polarizability is dispersionless. Since the SPP resonance in graphene is tunable by changing the Fermi level in this material, it is possible to achieve a double resonance with particles possessing resonant bare polarizability, e.g., due to polar optical phonons. In this case, the absorption of the EM radiation by such particles in the vicinity of the resonance frequency will be enhanced.

In the case of particles whose bare polarizability is frequency-independent in the considered THz range, several effects that are potentially interesting for applications can be achieved, such as (i) launching of SPPs with metal antennas for nanoscale graphene plasmonic circuits and devices [32,33,52] [note that a single spherical particle can help launch SPP modes with angular momenta $l = 0$ or 1 by choosing an appropriate polarization of the incident wave; see Eq. (29)]; (ii) scattering and localization of surface plasmons [53]; (iii) enhanced absorption of THz radiation in graphene [31,54]; (iv) enhanced transmission of the EM radiation through doped graphene in a "transparency window" determined by the surface plasmon resonance at a frequency corresponding to the SPP wave vector $q \sim h^{-1}$ (h is the particle's distance from graphene). These effects can be made broadband if several layers of particles are used for which the resonance frequencies should be somewhat different due to the different distances h of such layers to the graphene sheet. Finally, we would like to emphasize that, even though we exemplified the predicted effects with micrometer-

sized gold spheres, the localized plasmon resonance in these particles is irrelevant and their bare polarizability at the THz frequencies is nearly real and constant, $\alpha_0 \approx 4\pi\varepsilon_0 R^3$. In principle, particles made of a dielectric with a sufficiently high permittivity or even spherical holes in a capping dielectric layer could be used instead, even though α_0 would be smaller in this case, and one would require higher particle's concentrations to obtain considerable effects. On the theoretical side, it would be necessary to take into consideration particle-particle interactions [55].

APPENDIX A: INTEGRAL (22)

If one does not neglect the diffusion term, the integral (22) is given by

$$I = \frac{A}{4h^3} + \frac{B}{4h^2} - \frac{C}{2h} + \frac{aq_+ - b}{q_+ - q_-}e^{-2q_+h}$$
$$\times E_1(-2hq_+) - \frac{aq_- - b}{q_+ - q_-}e^{-2q_-h}E_1(-2hq_-), \quad (A1)$$

where

$$A = \frac{\varepsilon_2 - \varepsilon_1}{\varepsilon_2 + \varepsilon_1}, \quad B = \frac{2\varepsilon_1\sigma}{\varepsilon_0 D(\varepsilon_2 + \varepsilon_1)^2},$$
$$C = \frac{2\varepsilon_1\sigma^2}{\varepsilon_0^2 D^2(\varepsilon_2 + \varepsilon_1)^3},$$
$$a = \frac{2\varepsilon_1\sigma^3}{\varepsilon_0^3 D^3(\varepsilon_2 + \varepsilon_1)^4}, \quad b = \frac{2i\omega\varepsilon_1\sigma^2}{\varepsilon_0^2 D^3(\varepsilon_2 + \varepsilon_1)^3},$$

and $q_\pm$ are the roots of the polynomial

$$q^2 + \frac{\sigma}{\varepsilon_0 D(\varepsilon_2 + \varepsilon_1)}q - \frac{i\omega}{D}.$$

APPENDIX B: REFLECTION AND TRANSMISSION COEFFICIENTS

Considering the system schematically shown in the inset in Fig. 5, we write down the fields in three regions in the following way:

(1) $z \geqslant \delta = R + h$

$$H_y^{(1)} = e^{-ik(z-\delta)} - \hat{r}e^{ik(z-\delta)},$$
$$E_x^{(1)} = -e^{-ik(z-\delta)} - \hat{r}e^{ik(z-\delta)}; \quad (B1)$$

(2) $0 \leqslant z < \delta$

$$H_y^{(2)} = \hat{a} e^{-ik(z-\delta)} + \hat{b} e^{ik(z-\delta)} \, ,$$
$$E_x^{(2)} = -\hat{a} e^{-ik(z-\delta)} + \hat{b} e^{ik(z-\delta)} \, ; \tag{B2}$$

(3) $z < 0$

$$H_y^{(3)} = \hat{t} e^{-ikz} \, , \quad E_x^{(3)} = -\frac{\hat{t}}{\sqrt{\varepsilon_2}} e^{-ikz} \, . \tag{B3}$$

By applying the boundary conditions listed in Sec. VI, we obtain the following system of equations for the coefficients $\hat{r}$, $\hat{t}$, $\hat{a}$, and $\hat{b}$:

$$1 + \hat{r} = \hat{a} - \hat{b} \, ,$$
$$1 - \hat{r} = \hat{a} + \hat{b} + \frac{\sigma_{NP}^*}{\varepsilon_0 c}(1 + \hat{r}) \, ,$$

$$\hat{a} e^{-ik\delta} - \hat{b} e^{ik\delta} = \frac{\hat{t}}{\sqrt{\varepsilon_2}} \, , \tag{B4}$$
$$\hat{a} e^{-ik\delta} + \hat{b} e^{ik\delta} = \hat{t} + \frac{\sigma}{\varepsilon_0 c}(\hat{a} e^{-ik\delta} - \hat{b} e^{ik\delta}) \, .$$

In the limit $k\delta \to 0$, the system (B4) reduces to

$$1 + \hat{r} = \frac{\hat{t}}{\sqrt{\varepsilon_2}} \, ,$$
$$1 - \hat{r} - \hat{t} = \frac{\hat{t}}{\sqrt{\varepsilon_2}} \frac{(\sigma_{NP}^* + \sigma)}{\varepsilon_0 c} \, . \tag{B5}$$

from which the expressions (33) are obtained.

[1] *Metamaterials - Physics and Engineering Explorations*, edited by N. Engheta and R. W. Ziolkowski (IEEE Press, Piscataway, NJ, 2006).

[2] A. Boardman, V. Grimalsky, Y. Kivshar, S. Koshevaya, M. Lapine, N. Litchinitser, V. Malnev, M. Noginov, Y. Rapoport, and V. Shalaev, Laser Photon. Rev. **5**, 287 (2011).

[3] Z. Han and S. I. Bozhevolnyi, Rep. Prog. Phys. **76**, 016402 (2013).

[4] V. G. Kravets, F. Schedin, and A. N. Grigorenko, Phys. Rev. B **78**, 205405 (2008).

[5] V. E. Ferry, L. A. Sweadock, D. Pacifici, and H. A. Atwater, Nano Lett. **8**, 4391 (2008).

[6] F. J. Garcia de Abajo, Rev. Mod. Phys. **79**, 1267 (2007).

[7] T. Xu, Y.-K. Wu, X. Luo, and L. J. Guo, Nat. Commun. **1**, 59 (2010).

[8] M. Torrell, L. Cunha, Md. R. Kabir, A. Cavaleiro, M. I. Vasilevskiy, and F. Vaz, Mater. Lett. **64**, 2624 (2010).

[9] K. Kim, H. B. Lee, J. K. Yoon, D. Shin, and K. S. Shin, J. Phys. Chem. C **114**, 13589 (2010).

[10] L. Novotny and B. Hecht, *Principles of Nano-Optics* (Cambridge University Press, Cambridge, UK, 2006).

[11] *Metallic Nanoparticles*, edited by J. Blackman (Elsevier, New York, 2008).

[12] A. H. Castro Neto, F. Guinea, N. M. R. Peres, K. S. Novoselov, and A. K. Geim, Rev. Mod. Phys. **81**, 109 (2009).

[13] A. N. Grigorenko, M. Polini, and K. S. Novoselov, Nat. Photon. **6**, 749 (2012).

[14] Y. V. Bludov, A. Ferreira, N. M. R. Peres, and M. Vasilevskiy, Int. J. Mod. Phys. B **27**, 1341001 (2013).

[15] X. Luo, T. Qiu, W. Lu, and Z. Ni, Mater. Sci. Eng. R **74**, 351 (2013).

[16] Z. Q. Li, E. A. Henriksen, Z. Jiang, Z. Hao, M. C. Martin, P. Kim, H. L. Stormer, and D. N. Basov, Nat. Phys. **4**, 532 (2008).

[17] L. Ju, B. Geng, J. Horng, C. Girit, M. Martin, Z. Hao, H. A. Bechtel, X. Liang, A. Zettl, Y. R. Shen, and F. Wang, Nat. Nanotechnol. **6**, 630 (2011).

[18] A. Y. Nikitin, F. Guinea, F. J. Garcia-Vidal, and L. Martin-Moreno, Phys. Rev. B **85**, 081405 (2012).

[19] H. Yan, Z. Li, X. Li, W. Zhu, P. Avouris, and F. Xia, Nano Lett. **12**, 3766 (2012).

[20] S. Thongrattanasiri, F. H. L. Koppens, and F. J. García de Abajo, Phys. Rev. Lett. **108**, 047401 (2012).

[21] Z. Feng, Y. Wang, A. E. Schlather, Z. Liu, P. M. Ajayan, F. J. García de Abajo, P. Nordlander, X. Zhu, and N. J. Halas, Nano Lett. **14**, 299 (2014).

[22] O. L. Berman, V. S. Boyko, R. Y. Kezerashvili, A. A. Kolesnikov, and Y. E. Lozovik, Phys. Lett. A **374**, 4784 (2010).

[23] H. Yan, X. Li, B. Chandra, G. Tulevski, Y. Wu, M. Freitag, W. Zhu, P. Avouris, and F. Xia, Nat. Nanotechnol. **7**, 330 (2012).

[24] A. Y. Nikitin, F. Guinea, and L. Martin-Moreno, Appl. Phys. Lett. **101**, 151119 (2012).

[25] L. Gaudreau, K. J. Tielrooij, C. E. D. K. Prawiroatmodjo, J. Osmond, F. J. García de Abajo, and F. H. L. Koppens, Nano Lett. **13**, 2030 (2013).

[26] S.-A. Biehs and G. S. Agarwal, Appl. Phys. Lett. **103**, 243112 (2013).

[27] K. A. Velizhanin and A. Efimov, Phys. Rev. B **84**, 085401 (2011).

[28] Z. Chen, S. Berciaud, C. Nuckolls, T. F. Heinz, and L. E. Brus, ACS Nano **4**, 2964 (2010).

[29] G. Konstantatos, M. Badioli, L. Gaudreau, J. Osmond, M. Bernechea, F. P. G. de Arquer, F. Gatti, and F. H. L. Koppens, Nat. Nanotechnol. **7**, 363 (2012).

[30] P. A. Huidobro, A. Y. Nikitin, C. González-Ballestero, L. Martin-Moreno, and F. J. García-Vidal, Phys. Rev. B **85**, 155438 (2012).

[31] T. Stauber, G. Gómez-Santos, and F. J. García de Abajo, Phys. Rev. Lett. **112**, 077401 (2014).

[32] J. Chen, M. Badioli, P. Alonso-González, S. Thongrattanasiri, F. Huth, J. Osmond, M. Spasenović, A. Centeno, A. Pesquera, P. Godignon *et al.*, Nature (London) **487**, 77 (2012).

[33] Z. Fei, A. S. Rodin, G. O. Andreev, W. Bao, A. S. McLeod, M. Wagner, L. M. Zhang, Z. Zhao, M. Thiemens, G. Dominguez *et al.*, Nature (London) **487**, 82 (2012).

[34] A. V. Akimov, A. Mukherjee, C. L. Yu, D. E. Chang, A. S. Zibrov, P. R. Hemmer, H. Park, and M. D. Lukin, Nature (London) **450**, 402 (2007).

[35] K. Ray and J. R. Lakowitz, J. Phys. Chem. C **117**, 15790 (2013).

[36] M. Lunz, X. Zhang, V. A. Gerard, Y. K. Gunko, V. Lesnyak, N. Gaponik, A. S. Susha, A. L. Rogach, and A. L. Bradley, J. Phys. Chem. C **116**, 26529 (2012).

[37] R. Schreiber, J. Do, E.-M. Roller, T. Zhang, V. J. Schüller, P. C. Nickels, J. Feldmann, and T. Liedl, Nat. Nanotechnol. **9**, 74 (2014).

[38] D. E. Gomez, R. C. Vernon, P. Mulvaney, and T. J. Davis, Nano Lett. **10**, 274 (2010).

[39] Y. V. Bludov and M. I. Vasilevskiy, J. Phys. Chem. C **116**, 13738 (2012).

[40] S. A. Mikhailov and K. Ziegler, Phys. Rev. Lett. **99**, 016803 (2007).

[41] B. N. J. Persson and N. D. Lang, Phys. Rev. B **26**, 5409 (1982).

[42] J. D. Jackson, *Classical Electrodynamics* (J. Wiley, New York, 1998).

[43] M. M. Wind, J. Vlieger, and D. Bedeaux, Physica A **141**, 33 (1987).

[44] *Handbook of Mathematical Functions*, edited by M. Abramowitz and I. A. Stegun (Dover, New York, 1972).

[45] The expression for this integral without neglecting the diffusion term is given in Appendix A.

[46] P. Y. Yu and M. Cardona, *Fundamentals of Semiconductors* (Springer, Berlin, 1996).

[47] M. Hamma, R. P. Miranda, M. I. Vasilevskiy, and I. Zorkani, J. Phys. Condens. Matter **19**, 346215 (2007).

[48] G. Chumanov, K. Sokolov, B. W. Gregory, and T. M. Cotton, J. Phys. Chem. **99**, 9466 (1995).

[49] Here we extend our consideration beyond the electrostatic approximation where the magnetic field was neglected.

[50] M. Born and E. Wolf, *Principles of Optics* (Pergamon Press, Oxford, 1980).

[51] T. W. Ebbesen, H. J. Lezec, H. F. Ghaemi, T. Thio, and P. A. Wolff, Nature (London) **391**, 667 (1998).

[52] P. Alonso-González, A. Y. Nikitin, F. Golmar, A. Centeno, A. Pesquera, S. Vélez, J. Chen, G. Navickaite, F. Koppens, A. Zurutuza *et al.*, Science **344**, 1369 (2014).

[53] E. G. Mishchenko, Phys. Rev. B **88**, 115436 (2013).

[54] T. J. Echtermeyer, L. Britnell, P. K. Jasnos, A. Lombardo, R. V. Gorbachev, A. N. Grigorenko, A. K. Geim, A. C. Ferrari, and K. S. Novoselov, Nat. Commun. **2**, 458 (2011).

[55] R. M. Pereira, P. Pereira, G. Smirnov, and M. I. Vasilevskiy, Europhys. Lett. **102**, 67001 (2013).